JOURNAL OF CATALYSIS 102, 126–139 (1986)

The Effect of Group IA Cations on CO Hydrogenation over Ru/Y-Zeolites

RACHID OUKACI,[1] ABDELHAMID SAYARI,[2] AND JAMES G. GOODWIN, JR.[3]

Department of Chemical and Petroleum Engineering, University of Pittsburgh, Pittsburgh, Pennsylvania 15261

Received February 15, 1986; revised June 17, 1986

Previous results for zeolite-supported Ru prepared by ion-exchange suggested a possible effect of the nature and concentration of the neutralizing cations in the zeolite on the catalytic properties of the metal. The interpretation of these results were complicated by the fact that a series of zeolites with different Si/Al ratios was used. This paper reports the results of a study of a series of RuY catalysts prepared from NH_4Y, LiY, NaY, KY, RbY, and CsY zeolites. The nature of the group IA cations was found to have little effect on chemisorptive properties and on the activity and chain growth probability in CO hydrogenation on Ru. However, the nature of the cations produced changes in secondary reactions of primary olefinic products as a result of differences produced during catalyst preparation in Ru distribution in the zeolite crystallites and of possible modifications of the acid sites generated during reduction of the Ru. © 1986 Academic Press, Inc.

I. INTRODUCTION

Among the metals which catalyze carbon monoxide hydrogenation, ruthenium is considered to be one of the most active (*1*). Its characteristics for the Fischer–Tropsch (F-T) synthesis have been the object of a number of investigations. Several studies (*1–6*) have provided evidence that the adsorption and catalytic properties of ruthenium for CO hydrogenation depend markedly on the nature of the material on which it is supported, especially in well-dispersed systems. Zeolites are one class of supports upon which much attention has been focused in the ongoing search for means by which the product selectivity of F-T catalysts may be controlled. Due to their equivalent high surface areas, high metal dispersion can be maintained on such supports (*7–10*). Owing to the incorporation of the metal particles in a geometrically restricted environment, zeolite-supported catalysts may exhibit shape selectivity (*11–15*), thus restricting the normal chain growth process which characterizes F-T catalysts. In addition, for many zeolite-based catalysts, owing to their acidic nature, secondary reactions such as isomerization, usually acid-catalyzed, can influence the product distribution (*16*).

Earlier studies in this laboratory (*17, 18*) have provided evidence that the adsorption stoichiometries and states of H_2 and CO on ruthenium can be significantly affected by the type of zeolite in which the metal is entrapped. The observed changes in adsorption as well as in the activity and selectivity of these catalysts (*9, 10, 19*) have been attributed mostly to modifications of the electronic structure of the metal particles as a result of metal–support interactions. Although these previous studies suggested ways in which the zeolite support might affect adsorption and catalytic properties of ruthenium catalysts, the trends for these support effects still remained somewhat inconsistent and ambiguous. Indeed,

---

[1] Permanent address: CERHYD, Route de Sidi-Moussa, Dar-El-Beida, Algiers, Algeria.

[2] Permanent address: Universite de Tunis, Faculte des Sciences, Departement de Chimie, 1060 Tunis-Le belvedere, Tunisia.

[3] To whom all correspondence should be addressed.

0021-9517/86 $3.00

at least as far as the activity of these catalysts is concerned, Jacobs *et al.* (*19*) found that the less acidic zeolites acted as promoters for CO hydrogenation. However, others have demonstrated just the opposite effect of support acidity (*20*) or have found no effect at all (*3*). In fact, such conflicting results are not so surprising since, in addition to particle size effects, a large number of parameters may change the environment of the metal particles encaged in zeolites and hence their adsorption and catalytic properties. Some zeolite properties, such as acidity, depend on constituent atoms or ions of the zeolite framework (*21*).

The present work was undertaken to investigate systematically the influence of alkali neutralizing cations on CO hydrogenation over ion-exchanged zeolite-supported ruthenium catalysts.

II. EXPERIMENTAL

Materials. The zeolites NaY and NH_4Y (84% exchanged) were obtained from Strem Chemicals. Extensive ion-exchange of NaY with alkali nitrates (Alfa Products, ultrapure) was carried out in order to obtain MY (M = Li, K, Rb, Cs) zeolites with an exchange level as high as possible. NaY was vigorously stirred at room temperature for 18 h in an aqueous solution containing a twofold equivalent excess of MNO_3. Repeated contacts and higher temperatures were used in the case of the large-sized cations. Finally, the MY samples were washed several times with distilled water and then dried at 323 K.

The Ru-loaded zeolites were prepared by ion-exchange with $Ru(NH_3)_6Cl_3$ (Strem Chemicals) which had been first dissolved in a very dilute hydrochloric acid aqueous solution (pH = 4.5). Subsequently, the solution was mixed with the required amount of a given zeolite and stirred continuously for 50 h at room temperature. The solid was then filtered, thoroughly washed with deionized water in order to free it of Cl ions, and dried in air for 24 h at 323 K.

The resulting ruthenium catalyst precursors were then decomposed under vacuum, while heating at 0.5 K min^{-1} up to 673 K. This temperature was maintained for 4–5 h. The samples were then reduced for 1 h in hydrogen at that maximum temperature. This decomposition method using vacuum has been shown to result in higher dispersions of the metal than that resulting from decomposition under flowing helium (*22*). This is especially the case when the ruthenium-zeolites contain large-sized cations such as Rb and Cs.

In order to compare properties of Ru/zeolite catalysts with a more conventional system, one silica-supported Ru sample was prepared following the ion-exchange method recently reported by Gay (*23*). A calculated amount of $RuCl_3 \cdot 1.5H_2O$ (Strem) was dissolved in 6 ml H_2O per gram of SiO_2 used and added to the SiO_2 (Strem) under vigorous shaking. Hydrazine hydrate (Fisher Scientific) (0.8 ml per gram of silica) was then added slowly in order to generate *in situ* Ru(II) ammine species (*24*). The mixture was stirred continuously for several hours, then washed with cold 1 *M* ammonia solution (Fisher), and dried at 373 K for 3 h. The pretreatment and reduction conditions were the same as previously described.

Catalyst characterization. The composition of the various catalysts obtained was determined by atomic absorption and flame-emission spectroscopy using a Perkin–Elmer 380 atomic absorption spectrometer, before and after exchanging the ruthenium. A quantitative analysis of Ru in all samples was also performed by atomic absorption. The method applied was essentially the same as that described by Fabec (*25*) with minor modifications. The crystallinity of the catalysts were examined by X-ray diffraction at various stages of preparation, pretreatment and after reaction.

Chemisorption of hydrogen and carbon monoxide were carried out at ambient temperature in a conventional volumetric apparatus where a vacuum of 1×10^{-6} Torr was achieved. Air Products UPC grade hydrogen and helium were passed through a liquid-nitrogen trap and carbon monoxide through a dry-ice trap before being admitted to their respective reservoirs. Helium was used for dead-volume determination. The prereduced catalyst (0.5–1 g) was evacuated at room temperature, heated slowly (0.5 K min^{-1}) to 673 K in the presence of ca. 300 Torr H_2, and held at that temperature for 2 h. The sample was then evacuated for 2 h at 673 K and cooled to room temperature. The total uptake of hydrogen or carbon monoxide was determined from 50 to 300 Torr and the linear part of the isotherm was extrapolated to zero pressure. For this first point of the isotherm, the system was allowed to equilibrate during 24 h; for the subsequent points equilibrium was reached in about 1 h. A second isotherm was performed in the same manner after evacuating the catalyst for a short period of time (ca. 5 min). The difference between the two isotherms, at zero pressure, gave the amount of irreversibly (strongly) chemisorbed hydrogen or carbon monoxide (*26, 27*).

Hydrogen chemisorption measurements were used to calculate the surface area assuming a stoichiometry of $H_{\text{irr}}/\text{Ru}_{\text{s}} = 1$ (*26*) and an average Ru surface area of 8.17 Å^2 (10 Å = 1 nm) (*28*). The relationship $d_{\text{p}} = 5/S\rho$, where ρ is the density of the metal and S the surface area of Ru per gram of Ru, was used to assess the average Ru crystallite size, d_{p}. The Ru dispersion was calculated by $D(\%) = (\text{Ru}_{\text{s}}/\text{Ru}_{\text{T}}) \times 100$.

Reaction studies. Fischer–Tropsch synthesis was carried out in a tubular microreactor made from a stainless-steel tube of $\frac{3}{16}$ in. diameter (1 in. = 2.54 cm). The reaction temperature was controlled by a thermocouple inserted into the catalyst bed. The prereduced catalyst (0.2–0.5 g) was loaded into the reactor and heated under a hydrogen stream of 3.6 liters/h. The temperature was ramped to 673 K at 2 K/min and held there for 2 h before cooling to reaction temperature. Ultrahigh purity H_2 and CO supplied by Air Products were passed through molecular sieve traps to remove water. Prior to passage through the molecular sieve trap, the hydrogen was passed through a Deoxo unit to react any oxygen present to water. Reaction was carried out at atmospheric pressure and 483–573 K using a 1 : 1 mixture of H_2/CO flowing at 2.4 liters/h. Under these conditions, CO conversion was found to be lower than 10%, even at the highest temperatures used in this study. After 5 min of reaction, a sample of the effluent gas was analyzed on-line using two chromatographs. A Varian 3700 gas chromatograph fitted with a flame ionization detector and a 12 m SP-1700 column maintained at 353 K permitted separation of all hydrocarbons and most isomers in the C_3–C_6 fraction. A second chromatograph (Varian 1400) equipped with a thermal conductivity detector and a 2-m stainless-steel column packed with Porapak Q was used to separate CO, CO_2, CH_4, C_2H_4, C_2H_6, and H_2O. Peak areas were determined by an electronic integrator (Varian CDS 111). The hydrogen bracketing technique, which gave the catalyst a 30-min hydrogen exposure after every 5 min of reaction, was found sufficient to maintain a clean metallic surface, thus giving reproducible results.

TABLE 1

Unit Cell Composition of the Alkali Y-Zeolites

Zeolites	Composition
NaY[a]	$Na_{52}(AlO_2)_{52}(SiO_2)_{140}$
LiY	$Na_{36.4}Li_{15.6}(AlO_2)_{52}(SiO_2)_{140}$
KY	$Na_{2.6}K_{49.4}(AlO_2)_{52}(SiO_2)_{140}$
RbY	$Na_{20.3}Rb_{34.8}(AlO_2)_{52}(SiO_2)_{140}$
CsY	$Na_{21.8}Cs_{35.3}(AlO_2)_{52}(SiO_2)_{140}$

[a] Starting material.

III. RESULTS AND DISCUSSION

Chemical Composition and Structural Character of the Zeolites

The dehydrated unit cell composition of the various zeolites is given in Table 1. The metal loading of the ruthenium-exchanged zeolites is given in Table 2 with the chemisorption results. Except for LiY-zeolite, maximum amounts of exchange reported in the literature (*29*) were obtained for the other alkali zeolites. Chemical analysis after Ru exchange indicated that only 50% of the lithium exchanged remained in the zeolite. However, as will be seen in the following sections, even this small amount of lithium was sufficient to produce noticeable changes in the acid-catalyzed secondary reactions occurring during CO hydrogenation.

The X-ray diffraction measurements showed that the samples were highly crystalline. Furthermore, the X-ray diffractograms indicated that the structures of the zeolites were essentially unaffected by the various steps of catalyst preparation, reduction procedure, and reaction conditions. This is in agreement with the X-ray diffraction results reported by Pearce *et al.* (*30*) for the Ru/Y-zeolite system.

Relatively high values of nitrogen physisorption capacities obtained for the various catalysts before and after Ru exchange and reduction also indicated preservation of crystallinity with no loss of internal surface area due to breakdown of the zeolite framework during the preparation and reduction of the catalysts (*31*).

H_2 and CO Chemisorption

The hydrogen chemisorption measurements were used to calculate metal particle size and dispersion. However, H_2 chemisorption alone may not be very reliable for characterization when the metal is highly dispersed on acidic supports such as zeolites (*8*). With such supports, the suppression of hydrogen chemisorption may be significant. CO chemisorption has also been shown to be inadequate for surface area determination, since the stoichiometry for CO adsorption varies with Ru particle size (*32, 33*). However, CO adsorption can be used to compare relative metal dispersions and the presence of H_2 chemisorption suppression, since suppression of CO chemisorption appears to be less significant than that of H_2 (*18*). From consideration of CO/H and $CO/Ru_{(total)}$ ratios, it is possible to tell whether suppression of hydrogen chemisorption has taken place on Ru catalysts.

TABLE 2

Catalyst Characteristics Based on Hydrogen Chemisorption

Catalyst	Ru (wt%)	H_2 (irr.) (mol/g · cat.)	D (%)	d_p (Å)
RuHY	3.8	57	30	28
RuLiY	3.4	89	53	16
RuNaY	3.8	126	67	12
RuKY	3.2	83	52	16
RuRbY	3.6	87	49	17
RuCsY	3.7	102	56	15
$RuSiO_2$	1.8	48	53	16

The results of H_2 and CO chemisorption for the various Ru catalysts are given in Tables 2 and 3. As estimated by hydrogen chemisorption, the average diameters of the ruthenium particles, formed in the various alkali cation type Y-zeolites, were at or slightly above the upper limit of the supercage diameter (13 Å). Several interpretations can be found in the literature to explain such relatively large particle sizes. First, it is known that RuO_2 is readily formed at ambient temperature in air from small metal particles and that it is highly mobile. Upon heating, the ruthenium dioxide may migrate to the external surface of the zeolite where larger crystallites could

TABLE 3

CO Chemisorption Results

Catalyst	CO (irr.) (mol/g · cat.)	CO/H	$CO/Ru_{(total)}$
RuHY	404	3.5	1.1
RuLiY	665	3.7	2.0
RuNaY	924	3.7	2.5
RuKY	567	3.4	1.8
RuRbY	640	3.7	1.8
RuCsY	725	3.6	2.0

be formed (*8, 30*). If some metal exists as large particles on the external surface of the zeolite, an average metal particle diameter larger than the size of the zeolite pores would be calculated from chemisorption measurements, even though most of the metal might exist as very small particles inside the zeolite. Such a situation has been observed by TEM for highly dispersed Ru/NaY catalysts (*26*). Second, Pearce *et al.* (*30*) have observed by X-ray methods that, for ruthenium-exchanged zeolites pretreated under vacuum then reduced, up to 18% of the metal is atomically dispersed in the sodalite cages. Since, at room temperature, this ruthenium is inaccessible for hydrogen chemisorption, the average particle size calculated from hydrogen chemisorption is larger than the actual. Furthermore, localized destruction of the lattice to form cracks and holes has been observed by Verdonck *et al.* (*8*). Thus encapsulation of Ru clusters of intermediate size in these holes would also result in low dispersion being measured. Gustafson and Lunsford (*34*) have also suggested that in the presence of H_2 the mobility of Ru is increased, resulting in the agglomeration of Ru in several adjacent unit cells where the particles may be connected through the windows of the zeolite framework. This would render some portions of the metal particles inaccessible to hydrogen adsorption. Finally it has been reported that suppression of irreversible hydrogen chemisorption could be significant for most zeolite-supported ruthenium catalysts prepared by ion-exchange, resulting in an overestimation of the average particle diameter (*18*). The concentration and strength of acidic hydroxyl protons (correlated with the Si/Al ratio) are suggested to be the reason for this hydrogen chemisorption suppression. Luckily, the CO/H ratio has been shown to be a good indication of H_2 chemisorption suppression (*18*). Furthermore, CO/H ratios have been found in previous studies (*9, 33*) to be a function of particle size.

A comparison of the dispersions given in Table 2 with the CO/H ratios in Table 3 suggests that the dispersions of the ruthenium in the various Y-zeolites were high and similar, except for RuHY. The latter had higher concentration of acidic hydroxyl groups than the alkali cation neutralized zeolites. Thus, the suppression of hydrogen chemisorption would be expected to be more significant with RuHY, resulting in a much higher CO/H ratio than that normally found for a dispersion of Ru of 30% (*33*). A consideration of $CO/Ru_{(total)}$ for this catalyst suggests that the metal dispersion of this catalyst was in effect lower than that of the other Ru catalysts.

Catalytic Activity

The turnover frequencies (TOF) for the various catalysts studied were calculated using the estimated site concentrations provided by hydrogen chemisorption measurements. Because of the possible suppression of hydrogen chemisorption on zeolite-supported catalysts prepared by ion exchange, chemisorption measurements may not provide an exact measure of the metal dispersion and of the active ruthenium sites. Thus, the calculated TOF's based on hydrogen chemisorption and summarized in Table 4, should be considered as maximum values. Table 4 compares the TOF's at 523 K for CO conversion on the various catalysts.

No significant effect of the nature of the neutralizing alkali cations on TOF was

TABLE 4

Catalytic Properties of Ru Catalysts at 523 K

Catalyst	CO conversion (%)	TOF ($s^{-1} \times 10^3$)	E_a (kJ/mol)
RuHY	8.3	40.5	74.5
RuLiY	3.4	10.7	67.3
RuNaY	3.1	6.9	66.1
RuKY	2.3	8.0	80.7
RuRbY	4.4	14.1	100.6
RuCsY	4.5	12.4	100.1
$RuSiO_2$	1.5	8.8	99.7

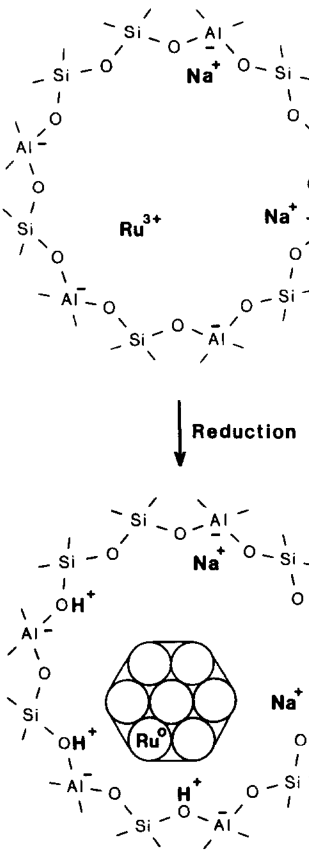

FIG. 1. Reduction scheme of ion-exchanged Ru/zeolites.

found, and the TOF's measured do not differ markedly from that of Ru/SiO_2. Having similar metal loadings, the concentration of the structural groups, formed during the reduction of the ruthenium ions in LiY, NaY, KY, RbY, and CsY, should be comparable in all these catalysts. This occurs since during ion-exchange, alkali cations M^+ ($M^+ = Li^+, Na^+, K^+, Rb^+, Cs^+$) are replaced by Ru ions:

$$m[Ru(NH_3)_6]^{3+} + 3mCl^- + nM^+[Y] \rightarrow [Ru(NH_3)_6]^{3+}_m M^+_{(n-3m)}[Y] + 3mMCl$$

The reduction step leads then to the simultaneous formation of acid sites, as illustrated in Fig. 1 where the complex ion $[Ru(NH_3)_6]^{3+}$ is shown as Ru^{3+} for simplicity.

It is generally accepted that for alkali cation zeolites, exchange of sodium ions for smaller or larger cations produces a change in the electrostatic field inside the zeolite, and hence a change in the strength of their acid sites (*21, 35*). As shown in Table 5 adapted from Ref. (*36*), the larger the charge-to-radius ratio, the greater will be the electrostatic field, hence the stronger the acidity. Considering the results in Table 4 then, for monovalent cations such as Li^+, Na^+, K^+, Rb^+, and Cs^+, either the variation in the acidity of the zeolites remain too small to produce significant differences in the activity of supported Ru or, as will be discussed later, the olefinic products may "neutralize" the acid sites, rendering them ineffective for electronic interactions with the metal particles. However, the TOF obtained for RuHY is four times greater than that for the other catalysts. This high activity of RuHY cannot be attributed only to an overestimation of metal particle size calculated from H_2 chemisorption. Assuming a similar dispersion to that for RuNaY, the TOF for RuHY still remains greater by at least a factor of 2. A possible metal–support interaction which increases the TOF of CO conversion on Ru sites in HY zeolite could be suggested.

Several workers have observed a similar trend of increasing activity for CO hydrogenation with increasing acidity of the support. Fajula *et al.* (*37*) found a higher activity for methanation on PdHY than on

TABLE 5

Physical Parameters for the Various Cationic Y-Zeolites[a]

Zeolite	Ionic radius (Å)	Electrostatic field (V/Å)	Electrostatic potential ($Å^{-1}$)
LiY	0.6	2.1	1.67
NaY	0.95	1.3	1.05
KY	1.33	1.0	0.75
RbY	1.48	0.8	0.67
CsY	1.69	0.6	0.59

[a] From Ref. (*36*).

PdNaY catalysts. They suggested a participation of acid sites of the support in CO hydrogenation. Similarly, Arai (*38*) found that the activity for F-T reactions was higher for RhHY than for RhNaY. Vannice (*39*) has also suggested that increasing the acidity of the support produces an increase in methanation activity of palladium. Leith (*20*) reported that, when sodium ions in Y-zeolites were exchanged by multivalent cations or protons, a two- to threefold increase in the specific activity of Ru resulted.

In all the works reviewed above, the enhancement of the activity of the metal, be it Pd, Rh, or Ru, in more acidic zeolites was attributed to an increase in the surface concentration of less strongly bound carbon monoxide species, resulting from an electron-deficient character of the supported metal which increased with the acidity of the support. Several research groups have examined the infrared spectra of CO adsorbed on Pd (*40*), Rh (*38*), and Ru (*17*) catalysts and found evidence that an increase in strength of the support acidity produces a shift to higher frequency and an enhancement of bands assigned to linearly adsorbed CO. It has been suggested that the presence of electron-acceptor sites on the support, i.e., the acidic hydroxyl groups, produces some electron depletion at the metallic surface and hence a decrease in the availability of *d*-electrons for back donation. These results are consistent with the suggestions by Vannice (*1*) and Okuhara *et al.* (*41*) that a weakening of the metal–carbon monoxide bond, paralleled by an increase in hydrogen adsorption, results in a higher activity for CO hydrogenation. However, such an interpretation for these results may be doubtful when one considers that the electron deficient character of the metal particles would also result in significant suppression of hydrogen chemisorption (*18*). In addition, Romannikov *et al.* (*42*), based on IR studies of coadsorption of CO and 1-hexene, have suggested that in the presence of electron-donating molecules such as olefins, the electron-deficient character of the metal particles may disappear as a result of interactions of the olefin molecules with the electron-acceptor sites of the zeolite, i.e., the acidic sites. As olefins are one of the major primary products of CO hydrogenation, they would act to "neutralize" the acid sites of the zeolite, thus interrupting the interaction of these acid centers with the metal particles according to the scheme:

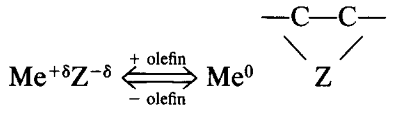

Thus, if such a mechanism is indeed operative, one must be cautious in trying to correlate the catalytic properties of a supported metal with IR results for CO adsorption alone. Such a phenomenon of adsorption "neutralization" would also explain why no effect of the nature of the neutralizing alkali cation on TOF was observed, even though these cations produce variations in the acid strength of the protonic sites, detected by the secondary acid-catalyzed reactions (*43*).

As for the higher activity observed for RuHY in CO hydrogenation, another interpretation may be proposed. It has been shown (*44*) that when Fischer–Tropsch reaction is carried out on a composite catalyst consisting of a physical mixture of CO hydrogenation component and an acid component (a zeolite), CO conversion is increased. This synergistic effect is provided by the presence of the acid sites of the zeolite which remove reaction intermediates formed on the F-T component by converting them to new species inert for further readsorption and chain growth on the metal sites. Thus, for RuHY, because of its higher concentration and strength of acid sites, the same "drain-off" mechanism must be in effect, resulting in the higher overall activity of this catalyst. However, this increase in activity is probably due in large part to the fact that the Ru particles were significantly large in this catalyst. It is

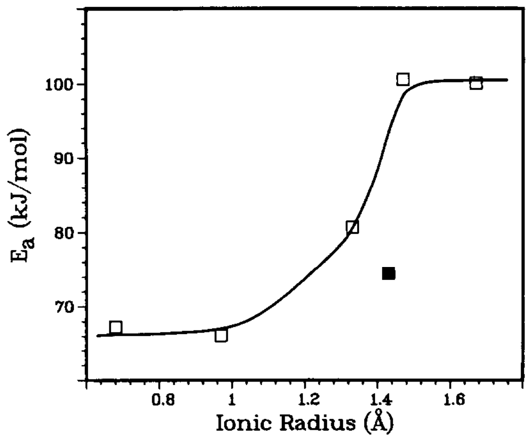

FIG. 2. Variation in E_a with neutralizing cation radius. (■) RuHY.

well known that TOF increases dramatically with Ru particle size in the range 1–4 nm (*9*).

The apparent activation energy for CO conversion, E_a, varied with the neutralizing cation (Table 4). While the values of E_a for RuRbY and RuCsY were equal to that for Ru/SiO$_2$ and are comparable to common values in the literature, the values for the other zeolite-supported catalysts were significantly lower. Values as low as 66 KJ/mol suggest some possible mass transport limitations. An explanation can be offered to the cause of this variation in E_a. Figure 2 shows a plot of E_a versus the crystal ionic radius of the initial charge-balancing cations of the zeolites used for catalyst preparation. Since the Ru exchange to give ca. 3 wt% is not the maximum exchange possible and the exchanging solution becomes depleted in Ru, it is suggested that Ru is initially more uniformly distributed throughout the zeolite crystallites for the small cation zeolites. Because of the limitations on the diffusion of $[Ru(NH_3)_6]^{3+}$ in the larger cation zeolites, Ru is probably less uniformly distributed and ion exchanges preferentially in the external shell of the zeolite crystallites. This difference in distribution of the Ru, if true, would not seem to affect the percentage dispersion of the reduced metal but would affect the activation energy of reaction by introducing diffusion limitations on reactants and products for the zeolite catalysts having smaller neutralizing cations. E_a for RuHY is plotted versus the crystal ionic radius of NH_4^+ (1.43 Å), since Ru was initially exchanged with NH_4Y, and does not fall squarely on the relatively smooth curve through the results for the alkali zeolites. This is probably due to the fact that NH_4Y is fairly easy to decompose and possibly contained a mixture of H^+ and NH_4^+ neutralizing cations at the time of Ru exchange. This conclusion about possible diffusion limitations during reaction in RuHY, RuLiY, RuNaY, and RuKY is further confirmed by the nonlinearity of the Arrhenius plots for these catalysts above 523 K.

Methane Selectivity and Chain Growth Probability

The term selectivity used in the present paper refers to the weight percentage of the total CO reacted which was converted into a given hydrocarbon or group of hydrocarbons. Table 6 compares the hydrocarbon product distributions obtained at 523 K on the various catalysts, and Fig. 3 gives the selectivity for CH_4 as a function of reaction temperature. The product selectivity shift towards lower molecular weight hydrocarbons, especially methane, with increasing temperature is consistent with the behavior of classical Fischer–Tropsch catalysts and reflects the thermodynamics of the system.

TABLE 6

Product Distribution at 523 K

Catalyst	Selectivity (wt%)					
	C_1	C_2	C_3	C_4	C_5	C_6
RuHY	34.3	13.7	19.1	17.1	12.5	3.5
RuLiY	33.4	14.3	21.8	17.6	11.8	1.1
RuNaY	32.7	14.0	21.5	17.0	10.9	3.9
RuKY	30.7	13.7	23.5	15.8	11.0	5.2
RuRbY	33.5	14.4	22.0	15.3	9.7	5.1
RuCsY	36.1	13.2	21.6	15.1	9.8	4.2

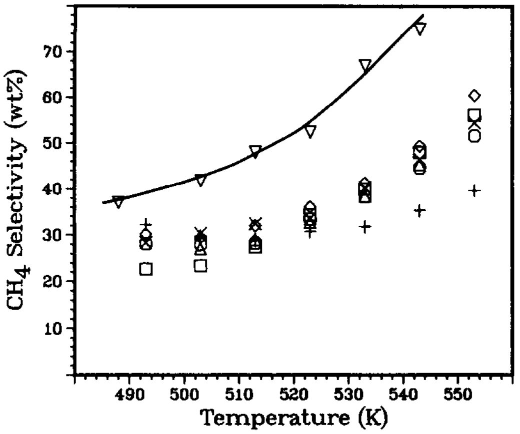

FIG. 3. Methane selectivity vs temperature. (□) RuHY, (○) RuLiY, (△) RuNaY, (+) RuKY, (×) RuRbY, (◇) RuCsY, (▽) Ru/SiO_2.

It is seen that, for the different Y-zeolite-supported Ru catalysts, the selectivity for CH_4 formation and the chain growth probability at 523 K were essentially the same regardless of the nature of the neutralizing alkali cations. Moreover, use of protons to neutralize the AlO_4^- groups of the zeolite did not seem to produce any significant change in CH_4 selectivity or chain growth probability. Therefore, a fundamental difference exists between the influence of alkali cations when used as neutralizing cations in a zeolite framework and their effect when added as promoters. In the latter case, it has been repeatedly shown (*16, 45*) that alkali promoters cause a shift to higher hydrocarbons at the expense of methane formation. Consequently, it may be concluded that neither the nature of the group IA cations (H^+, Li^+, Na^+, K^+, Rb^+, Cs^+) nor the total acidity has a substantial effect on chain growth, at least at atmospheric pressure. There are some more pronounced differences at higher reaction temperatures; however, no cation effect appears to be indicated.

In studying CO hydrogenation over a series of Ru/zeolites, Jacobs *et al.* (*19*) reported that under typical Fischer–Tropsch conditions ($H_2/CO = 1/1$, GHSV = 1800 h^{-1}, $T \sim 523$ K), RuNaX gave a higher selectivity for higher hydrocarbons than RuNaY did. This behavior was explained on the basis of a stronger metal–support interaction in the case of RuNaY due to the fact that NaY is more acidic than NaX. However, in the present work, RuHY and RuNaY exhibited the same selectivity for CH_4 despite the higher acidity (greater number of acid sites) of the former catalyst. Therefore, our results cannot be fully explained in the same terms as those employed in Ref. (*19*). The possible linkage between CH_4 formation and the acidity of the support, however, cannot be totally ruled out. Indeed, the correlation between the selectivity for methane and Si/Al ratio of the support (*10*) suggests that the relative amount of CH_4 formed is connected to the acid strength of the support rather than the total acidity. Indeed, Barthomeuf (*46*) has reported an excellent correlation between the acid strength of a series of zeolites and their Si/Al ratios. In addition, another important factor was stressed by this author: the nature of alkali cations as well as the partial or total decationization (replacement of the alkali cations by H^+) of a given zeolite induces a much less pronounced change in the acid strength than that brought about by a variation in Al content. This should explain why all the ion-exchange RuY zeolites gave almost the same selectivity for CH_4 and the same chain growth probability ($\alpha = 0.5$) regardless of the neutralizing cations.

Olefin Fraction

The C_3-fraction was selected for comparing the olefinic fractions yielded by the various catalysts, because, as expected (*3, 19*), the C_2-fraction was mainly paraffinic and the olefin fractions of hydrocarbons having more than three carbon atoms were complicated by possible secondary isomerization reactions.

In order to compare the ability of these catalysts to produce unsaturated hydrocarbons, the following question must be addressed: under which experimental conditions should the comparison be made?

TABLE 7

Cation Effect on Selectivity at Constant CO Conversion

Catalyst	T (K)	CO conv. (%)	C_1 (wt%)	$C_3^=/C_3^-$	i-C_4 (%)[a]
RuHY	503	4.5	23.4	2.3	58.2
RuLiY	533	4.5	38.3	2.00	23.5
RuNaY	533	4.0	38.4	2.9	16.2
RuKY	543	4.5	35.3	4.2	2.1
RuRbY	523	4.4	33.5	5.7	0.9
RuCsY	523	4.5	36.1	6.1	1.1

[a] % Isobutane in total C_4-fraction.

Previous workers have considered several situations. King (*3*) insisted mainly on constant CO conversion. Using as many as 16 supported Ru catalysts and despite some scatter in experimental data, he reported a unique inverse correlation between CO conversion and $C_3^=/C_3^-$ ratio. Only very few samples did not fit the correlation. Kikuchi *et al.* (*5*) reported two different plots of $C_3^=/C_3^-$ vs CO conversion for Ru/Al_2O_3 and Ru/V_2O_3. However, the data obtained with Ru on other supports does not fit either correlation. McClory and Gonzalez (*6*), using Ru/SiO_2 with various promoters, reported three types of comparisons where one of the following parameters was kept constant: temperature, CO conversion, or turnover number of CH_4 formation. They found that the first kind of comparison leads to larger differences between the catalysts. Morris *et al.* (*4*) varied the space velocity such that a constant conversion (10%) could be achieved at a given temperature (493 K). In the present work, the comparison was carried out both at constant temperature (523 K) and at constant CO conversion.

The nature of the neutralizing cations in Y-zeolites was found to have a strong influence on the olefin-to-paraffin ratio ($C_3^=/C_3^-$), regardless of whether the comparison was made at constant temperature (Fig. 4) or constant CO conversion (Table 7). Whether at constant temperature or conversion, the $C_3^=/C_3^-$ ratio was highest where the larger alkali cations had been exchanged into the zeolite and followed more or less the sequence Cs ~ Rb > K > Na > Li ~ H. The variation in the amount of isobutane in the C_4-fraction is included in Fig. 4 and Table 7 as this reflects the secondary acid-catalyzed reactions which were enhanced in the order: Cs ~ Rb < K ≪ Na < Li ≪ H. These results indicate that the major primary hydrocarbon products formed under the reaction conditions described above were olefins which could undergo either direct secondary hydrogenation on metal sites or secondary acid-catalyzed reactions. Furthermore, the nature of the alkali cations in the zeolites was found to have a considerable effect only on these secondary reactions, since the activity and chain growth probability remained practically constant whatever the nature of these cations.

Leith (*47*) has also observed that the olefin selectivity of zeolite-supported ruthenium in the hydrogenation of carbon monoxide is enhanced when potassium and cesium are exchanged into Y-zeolites. He interpreted his findings in terms of a lowering of the hydrogenation activity of the metal as a result of a decrease in the electron-deficient character of the metal particles brought about by the introduction of larger alkali cations into the support. However, this interpretation cannot fully ac-

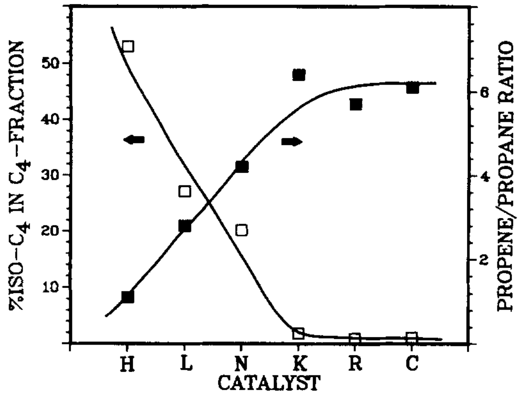

FIG. 4. Effect of neutralizing cation on olefin fraction and isobutane formation. Catalysts: (H) RuHY, (L) RuLiY, (N) RuNaY, (K) RuKY, (R) RuRbY, (C) RuCsY.

count for these results, since, if the electron-deficient character of the metal varied with the nature of the alkali cation, one would also anticipate an effect on both activity and chain growth probability. Except for RuHY which had a higher activity, no such effect was observed. Thus, one must look to other parameters which might possibly affect the olefin selectivity through changes in the nature of the alkali cation.

Ru particle size effects can certainly be ruled out completely since the hydrogen and carbon monoxide chemisorption results show that the dispersions of all the catalysts used in this study were similar, on the order of 50 to 60%. Furthermore, Kellner and Bell (*48*) have shown that the ratio $C_3^=/C_3^-$ is not dependent on particle size for dispersions below about 70%.

It has also been suggested (*49, 50*) that the hydrogenation activity of zeolite-supported metals may be enhanced under the action of the electrostatic field inside the zeolite acting directly on the reacting molecules rather than on the metal. As can be seen in Table 5, the difference in electrostatic field between LiY- and NaY-zeolites is much more important than between NaY and any other alkali Y-zeolite. Thus, if the electrostatic field were to have a major effect on the secondary reactions, one would expect to see a much more significant difference in olefin selectivities between Ru LiY and RuNaY and a less pronounced difference between RuNaY and the catalysts containing the larger alkali cations. However, this was not the case, since RuHY, RuLiY, and RuNaY had almost the same selectivity for olefins, and the $C_3^=/C_3^-$ ratios were two to three times higher for RuKY, RuRbY, and RuCsY. As pointed out previously, the polarizing power of the cations or the electrostatic field generated by them may have an effect on the strength of the Brønsted acid sites which would increase with decreasing cation radius (*35*). Although the variations in the strength of these acid sites with the nature of the cation are not significant enough to produce an electronic effect on the metal particles, they still may play an important role in the acid-catalyzed reactions. Thus, if the primary products of CO hydrogenation desorb mainly as olefins, as the results in Table 7 seem to indicate, these olefins may readsorb on metal sites to be further hydrogenated to paraffins. The rate of this reaction would remain unaffected by the nature of the alkali cations if the electronic structure of the metal particles is itself unchanged by the latter.

Olefins may also adsorb on the acid sites and undergo carbonium ion-type reactions. The most important proton-catalyzed reactions of olefins are isomerization, oligomerization, polymerization, disproportionation, paraffin formation via hydrogen-transfer, cracking, and coke formation. The rates of these reactions are influenced by the concentration and the acid strength of the hydroxyl groups present in the zeolite (*51, 52*). Thus, the decrease of the olefin-to-paraffin ratio with decreasing cation radius, paralleled by an increasing acidity strength, may be partly explained by a second olefin hydrogenation mechanism, i.e., the enhancement of hydrogen-transfer reactions catalyzed by acid sites. Formation of paraffins by similar hydrogen-transfer reactions have been observed in propylene polymerization over silica–alumina (*53*) and various olefin reactions on zeolites (*51, 54–56*). These studies of acid-catalyzed olefin reactions have demonstrated that the interaction of the acid hydroxyl groups with the adsorbed olefins is accompanied by olefin oligomerization. At temperatures higher than 370 K, the olefin oligomers decompose by a disproportionation mechanism to produce gaseous paraffins and some polyene species which remain on the zeolite (*51*). The gaseous paraffins produced from this oligomer decomposition are rich in isobutane and isopentane.

However, it is doubtful that the decrease in the $C_3^=/C_3^-$ ratio with decreasing cation radius can be accounted for completely by an enhancement of the hydrogen-transfer

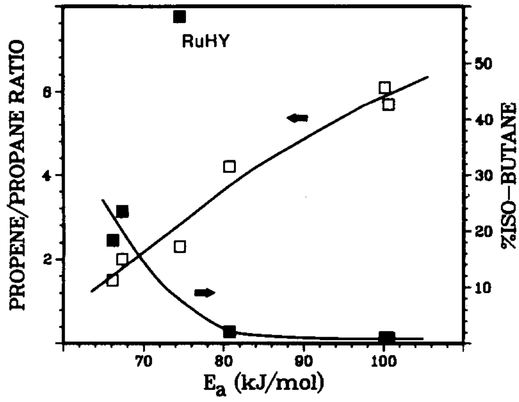

FIG. 5. Variation of $C_3^=/C_3^-$ ratio and i-C_4-fraction with E_a at constant conversion.

reactions as well as the disproportionation reactions of olefins with increasing support acidity. Otherwise, one would expect the hydrocarbon distribution with carbon number to be more different for RuHY, RuLiY, and RuNaY than for RuRbY and RuCsY. In addition, even though RuHY has a much larger concentration of acid sites than the other catalysts, it did not produce a $C_3^=/C_3^-$ ratio that was significantly out of line.

An important effect of mass transport limitations on the $C_3^=/C_3^-$ ratios due to a uniform versus shell distribution of Ru in the zeolite cannot be ruled out. The value of the activation energy can be used as an inverse measure of diffusion resistance during reaction. Figure 5 shows a plot of the $C_3^=/C_3^-$ ratio versus E_a for the zeolite-supported catalysts at constant conversion. This plot suggests a significant effect of diffusion on this ratio. Since hydrogenation of olefins is easy even during CO hydrogenation, the increase in residence time of olefins following their formation results in an increased probability for readsorption on the metal sites and hydrogenation. However, this interpretation is still not sufficient to explain the decrease of $C_3^=/C_3^-$ ratio with cation radius, since it has also been shown (*43*) that when all the protonic sites are replaced by K^+ in RuHY, the $C_3^=/C_3^-$ ratio increases from a low value of 2.6 to 16.9 for similar conversions. Such a result points again to the participation of acid sites in olefin hydrogenation.

It is thus suggested that, in addition to secondary hydrogenation on metal sites, the primary olefinic products may be hydrogenated significantly on the acid centers, the hydrogen being supplied not only by hydrogen transfer from adsorbed olefins but also by hydrogen spillover from the metal to the support.

Structural Isomerization

As mentioned earlier, the selectivity for isobutane in the C_4-fraction varied in the order Cs ~ Rb < K ≪ Na < Li ≪ H. Structural isomerization occurred primarily as a result of secondary reactions of olefins on the acid sites in the zeolites. As discussed in the previous section, formation of branched hydrocarbons from olefins can result from decomposition of oligomers formed on acid sites. Datka (*51*) has shown that the higher the concentration and strength of the acid sites in a zeolite, the more branched the olefin oligomers. Thus, a decomposition of the oligomer formed on the more acidic zeolites would result in the formation of more isoparaffins. Weeks and Bolton (*57*) have also demonstrated that the major products of 1-butene reaction on HY zeolite at 200°C are isobutane and isopentane formed by the breakdown of polymeric compounds.

The formation of isobutane via a bifunctional mechanism, i.e., direct isomerization of *n*-butenes to isobutenes on acid sites followed by hydrogenation on metal sites, is less likely, since the former reaction is known to be very slow compared to the carbonium ion-type reactions such as olefin oligomerization (*52*).

In order to gain insight into possible mass transfer effects on structural isomerization, a plot was made of the fraction of isobutane in the C_4-fraction versus E_a at constant conversion and is shown in Fig. 5. Since the formation of isobutane involves acid sites and since RuHY has a significantly greater number of acid sites than the other zeolite-supported catalysts, it may be expected that it would deviate from any trend established by the other catalysts. This appears to be the case, as is apparent in Fig. 5. Thus a possible effect of diffusion on structural isomerization, represented by the line in Fig. 5 for catalysts with comparable acid site concentrations cannot be completely ruled out. Steric factors may also influence olefin oligomerization in the presence of the larger cations such as K, Rb and Cs, thus inhibiting formation of the typical oligomer breakdown products such as isoparaffins.

There is also a good possibility that the nature of the alkali cations modified the properties of the acid sites. Certainly, the trend in selectivity for isobutane suggests this. Thus, at this time, it may be concluded that both modifications of the acid sites by the alkali cations and mass transfer effects may play a role in structural isomerization of olefins during CO hydrogenation.

Secondary acid-catalyzed reactions will be dealt with in more detail in a forthcoming paper (*43*).

IV. CONCLUSIONS

The results presented in this paper provide evidence that the nature of the cations used to neutralize the AlO_4^- groups of the zeolite can have a marked effect on the catalytic properties of ruthenium for CO hydrogenation in ion-exchanged zeolite-supported Ru catalysts. Although the nature of the neutralizing alkali cations in Y-zeolites has hardly any influence on the specific activity of the catalysts or on the overall chain growth probability, it has a pronounced effect on the olefin and branched hydrocarbon selectivities. Electronic and electrostatic field effects on reactions occurring on the metal particles may easily be ruled out. However, variations in the strength of the acid sites as a function of the nature of the neutralizing alkali cations as well as mass transfer limitations apparently play a major role in shaping the olefin and isoparaffin selectivities. Indeed, one probable reason for the variation of the olefin-to-paraffin ratio with the nature of the cation is the enhancement of olefin hydrogenation by a hydrogen-transfer mechanism on the acid sites following the decomposition of oligomers adsorbed on these sites. Spillover hydrogen may also enhance this process of olefin hydrogenation on the acid sites. The selectivity for isobutane, suggested to be formed by the breakdown of branched oligomers, was found to decrease with increasing cation radius. The variation in the strength of the acid sites generated during reduction as a function of the nature of the neutralizing alkali cations as well as steric factors are believed to have produced this effect. Finally, evidence suggests that the nature of the neutralizing cations in the zeolite can indirectly produce mass transfer effects during reaction as a result of effecting a uniform versus a shell distribution of Ru in the zeolites during catalyst preparation.

ACKNOWLEDGMENT

Funding for this research was provided by the U.S. Department of Energy, Office of Fossil Energy, under Grant DE-FG22-83PC60805.

REFERENCES

1. Vannice, M. A., *J. Catal.* **37,** 449 (1975).
2. Vannice, M. A., and Garten, R. L., *J. Catal.* **63,** 255 (1980).
3. King, D. L., *J. Catal.* **51,** 386 (1978).
4. Morris, S. L., Moyes, R. B., and Wells, P. B., *in* "Metal-Support and Metal-Additive Effects in Catalysis" (B. Imelik *et al.*, Eds.), p. 247. Elsevier, Amsterdam, 1982.
5. Kikuchi, E., Nomura, H., Matsumoto, M., and Morita, Y., *Appl. Catal.* **7,** 1 (1983).
6. McClory, M. M., and Gonzalez, R. D., *J. Catal.* **89,** 392 (1984).
7. Elliott, D. J., and Lunsford, J. H., *J. Catal.* **57,** 11 (1979).
8. Verdonck, J. J., Jacobs, P. A., Genet, M., and Poncelet, G., *J. Chem. Soc., Faraday Trans. 1* **76,** 403 (1980).
9. Chen, Y. W., Wang, H. T., and Goodwin, J. G., Jr., *J. Catal.* **83,** 415 (1983).
10. Chen, Y. W., Wang, H. T., and Goodwin, J. G., Jr., *J. Catal.* **85,** 499 (1984).
11. Nijs, H. H., Jacobs, P. A., and Uytterhoeven, J. B., *J. Chem. Soc., Chem. Commun.*, 1995 (1979).
12. Nijs, H. H., Jacobs, P. A., and Uytterhoeven, J. B., *J. Chem. Soc., Chem. Commun.*, 180 (1979).

13. Jacobs, P. A., *in* "Catalysis by Zeolites" (B. Imelik *et al.*, Eds.), p. 293. Elsevier, Amsterdam, 1980.
14. Ballivet-Tkatchenko, D., and Tkatchenko, I., *J. Mol. Catal.* **13,** 1 (1981).
15. King, D. L., Cusumano, J. A., and Garten, R. L., *Catal. Rev.-Sci. Eng.* **23,** 233 (1981).
16. Roper, M., *in* "Catalysis in C_1 Chemistry" (W. Keim, Ed.), p. 41. Reidel, Dordrecht, 1983.
17. Blackmond, D. G., and Goodwin, J. G., Jr., *J. Chem. Soc., Chem. Commun.,* 125 (1981).
18. Wang, H. T., Chen, Y. W., and Goodwin, J. G., Jr., *Zeolites* **4,** 56 (1984).
19. Jacobs, P. A., Verdonck, J. J., Nijs, H. H., and Uytterhoeven, J. B., *Adv. Chem. Ser.* **178,** 15 (1979).
20. Leith, I. R., *J. Catal.* **91,** 283 (1985).
21. Barthomeuf, D., *in* "Catalysis by Zeolites" (B. Imelik *et al.*, Eds.), p. 55. Elsevier, Amsterdam, 1980.
22. Oukaci, R., Sayari, A., and Goodwin, J. G., Jr., manuscript in preparation.
23. Gay, I. D., *J. Catal.* **80,** 231 (1983).
24. Allen, A. D., Harley, F. B., Harris, R. O., Reinsalu, V. P., and Senoff, C. V., *Inorg. Synth.* **12,** 3 (1970).
25. Fabec, J. L., *At. Spectrosc.* **4,** 46 (1983).
26. Goodwin, J. G., Jr., *J. Catal.* **68,** 227 (1981).
27. Sayari, A., Wang, H. T., and Goodwin, J. G., Jr., *J. Catal.* **93,** 368 (1985).
28. Dalla Betta, R. A., *J. Catal.* **34,** 57 (1974).
29. Breck, D. W., "Zeolite Molecular Sieves: Structure, Chemistry, and Use." Wiley–Interscience, New York, 1974.
30. Pearce, J. R., Mortier, W. J., and Uytterhoeven, J. B., *J. Chem. Soc., Faraday Trans 1* **75,** 1395 (1979).
31. Feng, D., M.S. thesis, 1985.
32. Dalla Betta, R. A., *J. Phys. Chem.* **79,** 2519 (1975).
33. Yang, C.-H., and Goodwin, J. G., Jr., *React. Kinet. Catal. Lett.* **20,** 13 (1982).
34. Gustafson, B. L., and Lunsford, J. H., *J. Catal.* **74,** 393 (1982).
35. Richardson, J. T., *J. Catal.* **9,** 182 (1967).
36. Ward, J. W., *J. Catal.* **10,** 34 (1968).
37. Fajula, F., Anthony, R. G., and Lunsford, J. H., *J. Catal.* **73,** 237 (1982).
38. Arai, H., *Nippon Kagaku Kaishi,* 192 (1982); *Chem. Abstr.* **96,** 125964f (1982).
39. Vannice, M. A., *J. Catal.* **40,** 129 (1975).
40. Figueras, F., Gomez, R., and Primet, H., *Adv. Chem. Ser.* **121,** 480 (1973).
41. Okuhara, T., Kimura, T., Kobayashi, K., Misono, M., and Yoneda, Y., *Bull. Chem. Soc. Jpn.* **57,** 38 (1984).
42. Romannikov, V. N., Ione, K. G., and Pederson, L. A., *J. Catal.* **66,** 121 (1981).
43. Oukaci, R., Sayari, A., and Goodwin, J. G., Jr., to be submitted for publication.
44. Chang, C. D., Lang, W. H., and Silvestri, A. J., *J. Catal.* **56,** 268 (1979).
45. Anderson, R. B., *in* "Catalysis" (P. H. Emmett, Ed.), Vol. 4. Reinhold, New York, 1956.
46. Barthomeuf, D., *J. Chem. Soc., Chem. Commun.,* 743 (1977), and references therein.
47. Leith, I. R., *J. Chem. Soc., Chem. Commun.,* 93 (1983).
48. Kellner, C. S., and Bell, A. T., *J. Catal.* **75,** 251 (1982).
49. Naccache, C., Kaufherr, N., Dufaux, M., Bandiera, J., and Imelik, B., *in* "Molecular Sieves II" (J. R. Katzer, Ed.), ACS Symp. Series, Vol. 40, p. 538. Amer. Chem. Soc., Washington, D.C., 1977.
50. Dalla Betta, R. A., and Boudart, M., *in* "Proceedings, 5th International Congress on Catalysis, Palm Beach, 1972" (J. W. Hightower, Ed.), p. 1329. North-Holland, Amsterdam, 1973.
51. Datka, J., *in* "Catalysis by Zeolites" (B. Imelik *et al.*, Eds.), p. 121. Elsevier, Amsterdam, 1980.
52. Guisnet, M., *in* "Catalysis by Acids and Bases" (B. Imelik *et al.*, Eds.), p. 283. Elsevier, Amsterdam, 1985.
53. Shephard, F. E., Rooney, J. J., and Kemball, C., *J. Catal.* **1,** 379 (1962).
54. Venuto, P. B., Hamilton, L. A., and Landis, P. S., *J. Catal.* **5,** 484 (1966).
55. Bein, Th., Plath, P. J., and Schulz-Ekloff, G., *React. Kinet. Catal. Lett.* **26,** 153 (1984).
56. Langner, B. E., *J. Catal.* **65,** 416 (1980).
57. Weeks, T. J., Jr., and Bolton, A. P., *J. Chem. Soc., Faraday Trans. 1* **70,** 1676 (1974).